SOIL SPRING CONSTANTS DURING LATERAL FLOW OF LIQUEFIED GROUND

Rolando ORENSE[1], Kenji ISHIHARA[2], Susumu YASUDA[3], Iwao MORIMOTO[4] And Masahiro TAKAGI[5]

SUMMARY

From the results of large-scale shaking table tests on real-size piles subjected to liquefaction-induced ground flow, the coefficient of subgrade reaction or soil spring constant was calculated. For comparison purposes, the results obtained from lateral loading test in unliquefied ground was also analyzed. Results showed that the reduction in soil spring constants for piles in sloping liquefied ground is the result of the increase in pore water pressure and the increase in the relative displacement between pile and ground. In addition, the magnitude of soil spring constant during liquefaction-induced flow ranges between 1/10~1/500 with respect to that of unliquefied ground

INTRODUCTION

Generally speaking, piles are employed to increase the performance of foundations at potentially liquefiable sites. However, recent large-scale earthquakes, such as the 1995 Hyogoken Nambu Earthquake, have shown that pile foundations are susceptible to earthquake damage due to the reduction in the stiffness of surrounding soils during seismic shaking as well as the associated lateral ground deformation induced by soil liquefaction. Rational design of pile foundations under seismic condition requires knowledge of the soil forces resulting from relative soil-pile displacement. In other words, the response of piles due to liquefaction is very sensitive to the soil restraint. The restraint offered by soil against the movement of buried structures is called the subgrade reaction (expressed as force per unit area of contact surface). The ratio between this pressure at any given point of the contact surface and the deflection produced is the coefficient of subgrade reaction or soil spring constant.

Based on studies made which are reflected in available literature, the response of pile foundations to lateral ground movements has been clearly understood for cases involving only dry cohesionless deposits (e.g., Audibert and Nyman, 1977; Trautmann and O'Rourke, 1985). However, based on observations from past earthquakes that liquefaction-induced permanent ground displacements have been the major cause of damage to pile foundations, a deeper insight into the liquefied soil-pile interaction is necessary for the earthquake resistant design and risk evaluation of these structures.

Liquefaction-related experiments dealing with the soil spring constant have been performed by several researchers. Yoshida and Uematsu [1978] performed experiments on model pile in liquefied ground and their results showed that the coefficient of subgrade reaction on pile decreased to around one percent or less of that in the non-liquefied ground. Matsumoto et al. [1987] observed that the subgrade reaction was in direct proportion to the effective overburden pressure and in inverse proportion to the square root of the relative displacement. On the other hand, experiments conducted by Yasuda et al. [1987] showed that the critical shearing force and the soil spring constant in the liquefied ground became less than ten percent of those in the non-liquefied ground. Kiku et al. [1995] performed tests in which a buried pipe was pulled in a model ground previously shaken until a prescribed excess pore water pressure was obtained. Their tests showed that the soil resistance decreased with

[1]   Kiso-jiban Consultants Co. Ltd., Tokyo, Japan Fax No:+81-3-5210-9405
[2]   Dept. of Civil Eng., Tokyo Science University, Tokyo, Japan Fax No: +81-471-23-9766
[3]   Dept. of Civil Eng., Tokyo Denki University, Saitama, Japan Fax No: +81-492-96-6501
[4]   Kiso-jiban Consultants Co. Ltd., Tokyo, Japan Fax No:+81-3-5210-9405
[5]   High Pressure Gas Safety Institute of Japan, Tokyo, Japan Fax No: +81-3-3438-4163

increase in pore water pressure, and during complete liquefaction, the soil resistance was reduced to 1/30 of the pre-shaking value.

It should be mentioned that the above tests were performed mostly on small-scale box with heights generally less than one meter. In addition, the lateral flow tests involved moving the pipe or pile within the liquefied ground. The low confining pressures in such small scale 1-g models may present problems in relation to pore pressure generation and dissipation, as well as in the stress-strain relations of the soil. In the present tests (see Yasuda et al., 2000 for further details), real-size piles having diameter of 20cm and length of 5m were employed. Moreover, as in the in-situ condition, the liquefied ground moved laterally while the piles are fixed at the bottom. Hence, the present tests overcome the problems associated with low confining pressures in small scale 1-g models, and therefore, the response of real-size piles in actual ground conditions can be properly simulated. Thus, the present tests have produced precious information which can be employed to evaluate the validity of various soil-spring models used in pile analysis, and can also be used to improve existing numerical methods and design guidelines for pile foundations in potentially liquefiable deposits.

From the results of the large-scale shaking table tests, the coefficient of subgrade reaction or spring constant for liquefied soil undergoing lateral flow is analyzed and compared with the case of unliquefied ground.

COMPUTATIONAL PROCEDURE

The procedure employed in the calculation of the spring constant is as follows. From the strains measured at several elevations within the pile, the curvature of the pile is calculated using the following equation:

$$\phi = \frac{\varepsilon_1 - \varepsilon_2}{d} \tag{1}$$

where ϕ is the curvature developed in the pile at the location of the strain gauges, ε_1 and ε_2 are the readings of the strain gauges attached to the two opposite sides at a particular section of the pile, and d is the diameter of the pile. To simplify the calculation, elastic condition is assumed and the bending moment at each point is obtained from the moment-curvature relations available for each pile type. The moment-curvature relations for the piles employed in this study are shown in Figure 1. In the figure, M_c denotes cracking moment, M_y is yield moment, M_u is ultimate moment and M_p is plastic moment. In order to have a smooth moment distribution, curve fitting is used where the moment function is interpolated through a polynomial function of appropriate degree.
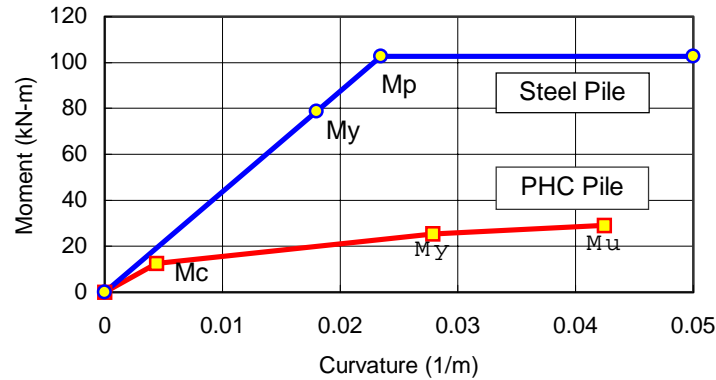
Figure 1: Moment curvature relations of piles used

From the known moment function, $M(z)$, where z is the axis along the pile, classical elastic beam theory is used, i.e., pile deflection, $\delta(z)$, is obtained by integrating the moment function while the soil reaction, $p(z)$, is calculated by differentiating the moment function. When the soil displacement distribution, $u(z)$, is known, the horizontal spring constant, $k(z)$, at any depth is easily calculated as follows:

$$k = \frac{p}{u - \delta} \tag{2}$$

Since the soil reaction, p, is expressed as force per unit area, while u and δ have units of length, the soil spring constant, k, has unit of force per volume.

The results of two tests are discussed below. The first test involved lateral load test on a PHC pile, where the soil spring constant of unliquefied ground was measured. The second test involved calculation of soil spring constants for two PHC piles and a steel pile subjected to liquefaction-induced lateral ground flow. Note that the values obtained in the first test are used to express the amount of reduction in spring constant as a result of liquefaction-induced flow.

RESULTS OF LATERAL LOAD TEST

In the lateral load test on the PHC pile conducted prior to shaking, forces in ten increments ranging from 4.9kN to 49kN, were applied slowly on the pile top and the pile top deflection as well as the strains at 12 levels within the pile were monitored. The load-displacement relations are depicted in Figure 2. For the purpose of the analysis, the pile response during each peak loading, i.e., at the time when the applied force is maximum, is considered and the bending moment, pile deflection, soil reaction and soil spring constant are evaluated at each of these peak points.
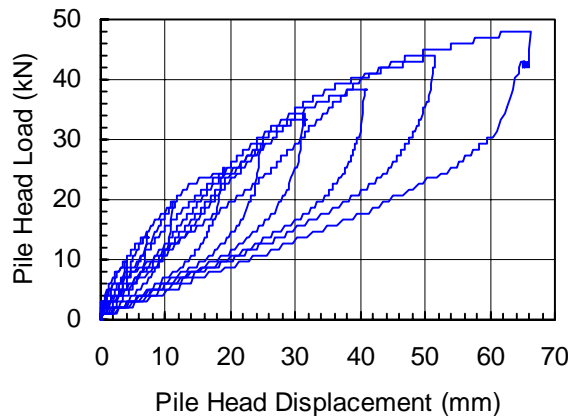
Figure 2: Force-displacement relation at the pile top (lateral load test)

Since the magnitude of k is sensitive to small values of δ, the spring constant is evaluated only on the upper 2m length of the pile where the deflection is large. This length is consistent with the value of $1/\beta$ where the spring constant should be evaluated as specified in the design code (e.g., Specification for Highway Bridges published by the Japan Road Association, 1996).

The vertical distributions of spring constant for various applied forces are shown in Figure 3(a). It can be seen that generally, there is an increase in the value of the spring constant with depth. Figure 3(b) shows the relation between the spring constant and the pile displacement. Although there is a wide scattering of data, the pattern can be represented by the solid line indicated in the figure. Hence, as the pile displacement increases, the spring constant decreases.

SOIL SPRING CONSTANTS DURING LIQUEFACTION-INDUCED FLOW

Overview of Test Results for Sloping Ground

Next, the test results for piles installed in a sloping liquefiable ground are analyzed. For further details regarding the test, refer to Yasuda et al. [2000]. In this test, one steel pile and three PHC piles were installed within a loose sand deposit with surface slope of around 14%. The model ground was shaken in two stages with sinusoidal wave of 250gals and frequency of 1Hz. Because of the initial sloping configuration of the ground, the liquefied ground moved towards the bottom of the slope, and induced lateral load on the piles.

The ground configuration at the end of the first shaking is depicted in Figure 4. Based on the movement of the surface markers, the maximum lateral displacement was in the order of around 30cm. From the figure, it is evident that the left side of the model (downslope) moved more compared to the right side (upslope). This is probably because of the presence of the steep slope on the right side of the model which induced some ground movement towards the right, i.e., against the direction of lateral flow. In addition, there is also the possibility that the thick unsaturated layer on the right side restrained the occurrence of flow.
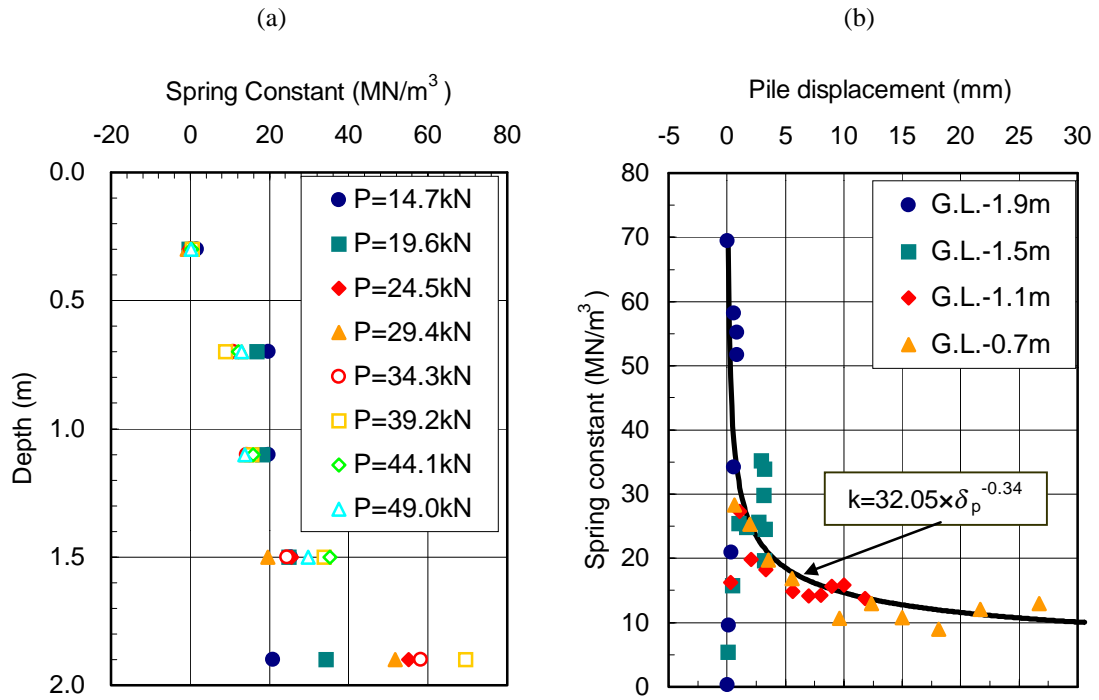
(a)

Spring Constant (MN/m³)

(b)

Pile displacement (mm)

$$k = 32.05 \times \delta_p^{-0.34}$$

Figure 3: (a) Variation of spring constant with depth; (b) Relation between spring constant and pile displacement (lateral load test)
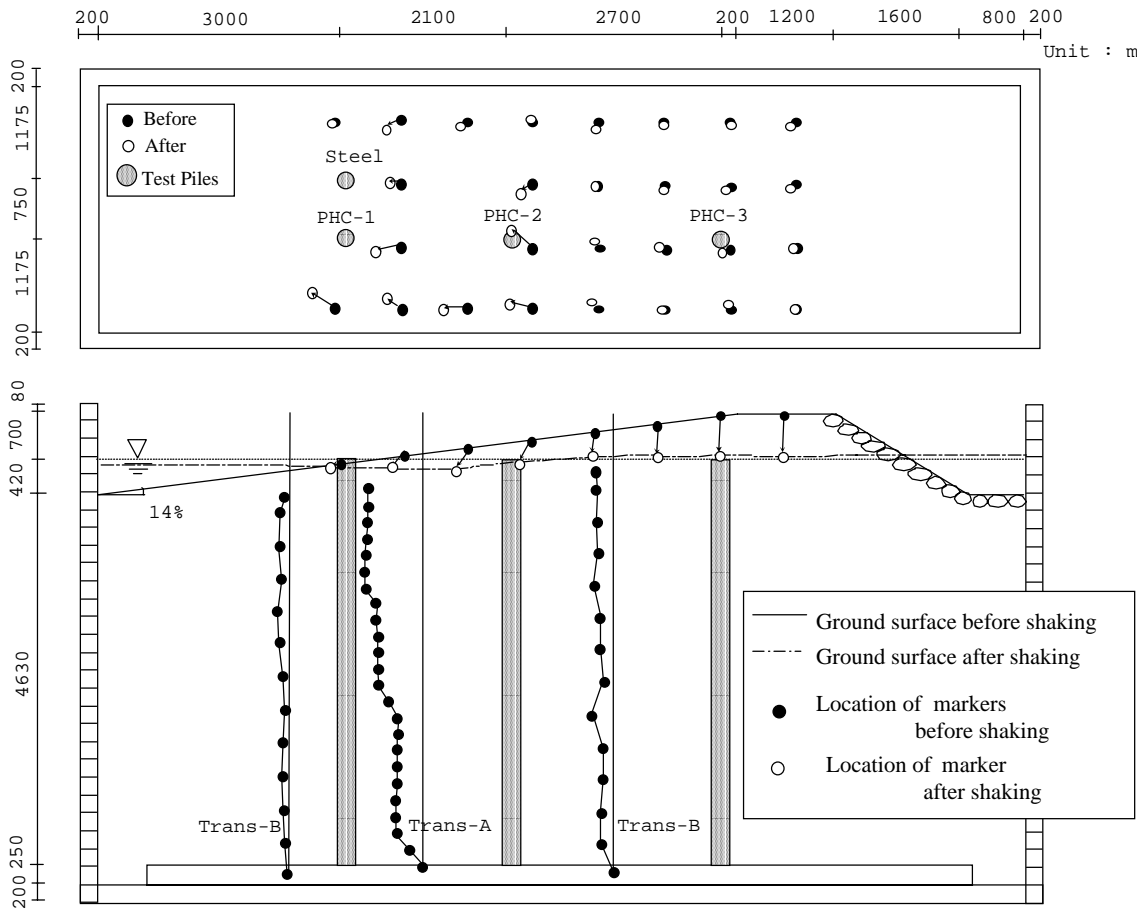
Unit : m

Figure 4: Ground deformation after the first shaking

It is also noted that the soil displacement obtained using shear displacement transducer A (Trans-A in Figure 4) is generally larger, with maximum value in the order of around 60cm near the ground surface. Moreover, the displacement distribution shows a ladder-type variation with depth, which indicates possible malfunctioning at several depths. On the other hand, the magnitudes of the ground surface displacement in the lower and upper portions of the slope as obtained using Type B transducer (Trans-B in Figure 4) are in the order of 10cm and 20cm, respectively. Although the patterns of measured soil movement with depth show kinks at various depths, these values are more reasonable compared to those obtained using Type A transducer. Thus, for the purpose of calculating the spring constant, only the readings obtained by Type B transducer are considered. Note that the readings obtained by this type of transducer may include panel deformation resulting from ground settlement; however, it is very difficult to subdivide the total reading into components induced by lateral flow and those caused by ground settlement. Hence, in the analysis presented herein, the monitored readings are considered as caused by lateral flow only.

Only the stage corresponding to the first shaking is considered in the analysis. This is because after the first shaking, the model ground became essentially flat, and substantial lateral ground movements were not observed in the subsequent shaking. Also, as mentioned earlier, the soil movement near the top of the slope is very small due to the presence of the steep slope on the right side of the model and therefore, analysis for PHC No.3 pile is complicated. Hence, only the results for the three piles (PHC No. 1, PHC No. 2 and steel piles) located on the lower portion of the slope are considered.
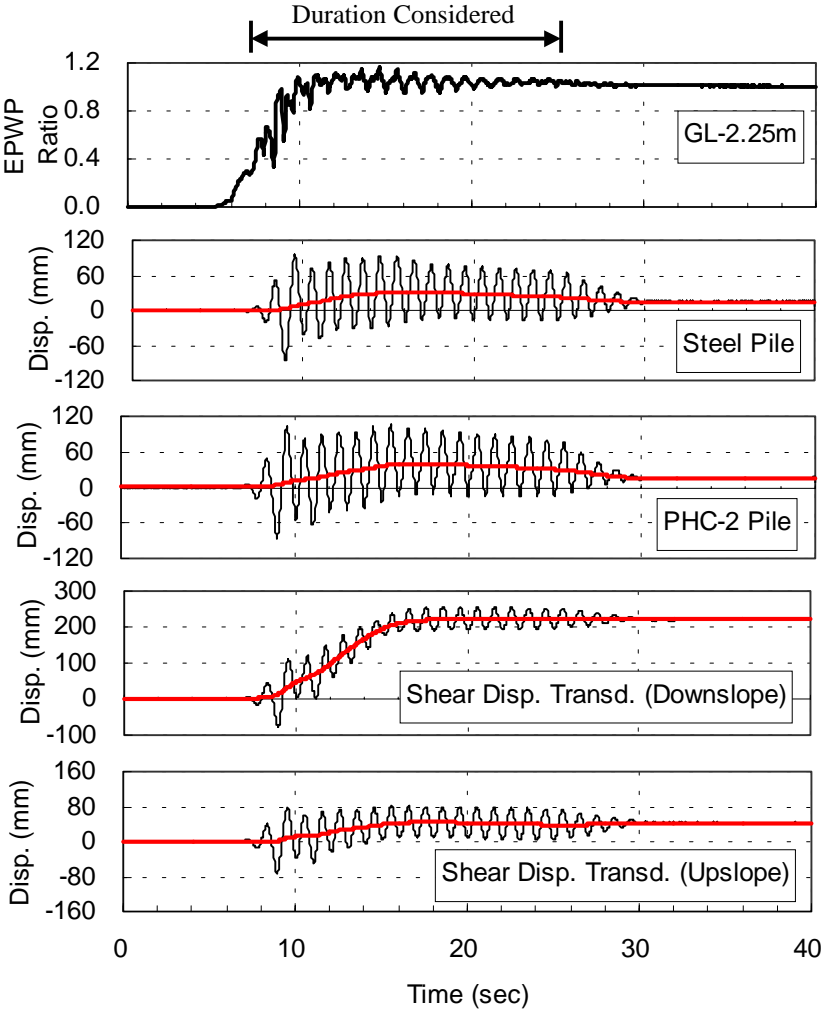

Figure 5: Time histories of excess pore water pressure ratio, pile top displacements of steel and PHC No.2 piles, and ground surface displacements from downslope and upslope shear displacement transducers

5

The time histories of excess pore water pressure ratio, pile top displacements, and ground surface displacements are shown in Figure 5. The pore water pressure started to increase from the beginning of shaking, reaching complete liquefaction (excess pore water pressure ratio, r_u, equals 1.0) in about 5sec thereafter. The displacement time histories consist of both cyclic (dynamic) and residual (static) components. The former is induced as a result of shaking while the latter is due to the lateral movement of the ground towards the bottom of the slope. Note that at the end of shaking, the cyclic components disappear as expected while residual displacements remained. Since the pile response due to the lateral movement of the ground is the main concern in this study, only the residual component is considered while the dynamic (cyclic) component is neglected. The residual components of the displacements are indicated in the figure by thick lines, and these were obtained by averaging the time histories. Moreover, the analysis is limited to the time interval when complete liquefaction occurred and the soil and the piles were in motion, as indicated in Figure 5. For simplicity, the various parameters are evaluated at ten time frames, i.e., between $t=7\sim25$ sec at intervals of 2sec.
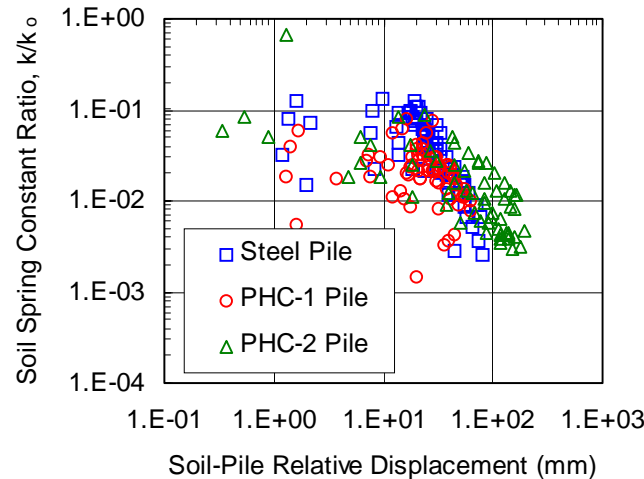
Calculation of Spring Constants

In the same way as in the lateral load test, the bending moment distributions of the three piles are calculated from the strain gauge readings. Since the piles are fixed at the bottom and free at the top, the moving soil induced zero bending moment at the top and large bending moment at the bottom. Because the calculated bending moment distributions near the bottom of the piles become complicated, the interpolation is confined only up to GL-3.5m. This is reasonable considering that the pile displacement near the bottom is small. Pile deflections were then calculated by integrating the bending moment functions. Moreover, the bending moment distribution is differentiated to obtain the distribution of soil reaction for each pile.

From the known pile deflection, $\delta(z)$, soil displacement, $u(z)$, and soil reaction, $p(z)$, the lateral soil spring constant, k, at specified depths can be calculated from Equation (2). The distribution of spring constant for the steel pile and PHC No.2 pile are shown in Figure 6. Note that these values of spring constant correspond to a completely liquefied condition. Due to the small magnitude of the relative soil-pile displacement near the bottom of the pile, the soil spring constants were calculated only on the top 3.5m of the pile. It can be seen from the figures that generally, the spring constant, k, during liquefaction-induced flow ranges between $0.01\sim0.60$ MN/m^3, and gradually increases with depth. In addition, the value of k generally decreases with time due to the fact that the relative displacement between soil and pile also increases with time within the time frame considered.
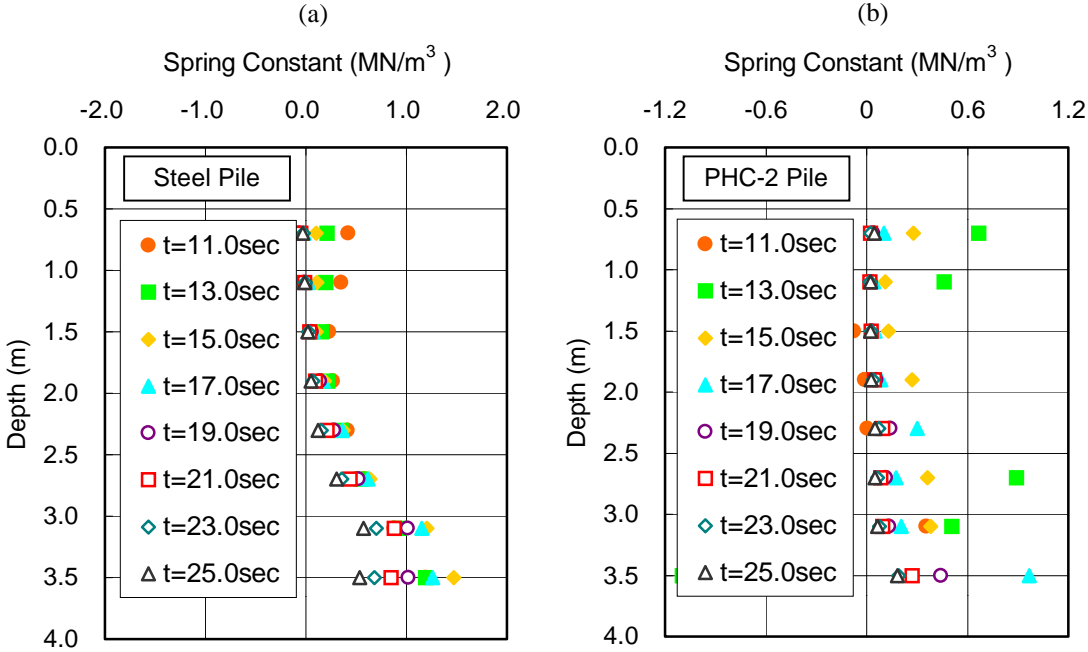
Figure 6: Distribution of soil spring constant with depth: (a) steel pile; (b) PHC No.2 pile

To analyze the reduction in spring constant as a result of liquefaction-induced flow, the k values shown in Figure 6 are normalized by the magnitude of the spring constant before liquefaction, k_o. For this purpose, the soil spring constant computed from the results of the lateral load test which was discussed earlier are employed to represent the condition corresponding to unliquefied ground. The plot showing the relation between the normalized spring constant and relative soil-pile displacement for the three piles are shown in Figure 7. The figure shows that the normalized spring constant, k/k_o, decreases as the relative displacement between the liquefied soil and the pile increases. Moreover, it can be seen that the soil spring constant during liquefaction-induced flow drops to around 1/10~1/500 of that in an unliquefied ground. Note that this reduction range seems valid for all piles studied, irrespective of whether it is a steel pile or a PHC pile.

Figure 7: Variation of normalized soil spring constant with relative displacement

CONCLUDING REMARKS

Shaking table test using a large-scale laminar shear box was performed to investigate the response of real-size piles during lateral flow of ground and to calculate the soil spring constant during liquefaction-induced lateral flow. The main conclusions obtained in the analysis of test results are as follows:

1. The results of the lateral load test on unliquefied ground show that the experimentally obtained spring constant increases with depth and decreases as the pile displacement increases.
2. The shaking table test showed that the soil spring constant of liquefied ground undergoing flow decreases as the magnitude of the relative displacement between soil and pile increases. Generally, the spring constant is reduced to around 1/10~1/500 of that in an unliquefied ground.

ACKNOWLEDGMENT

REFERENCES

1. Audibert, J.M.E. and Nyman, K.J. (1977), "Soil restraint against horizontal motion of pipes," *Journal of Geotechnical Engineering Division, ASCE*, Vol. 103, GT10, 1119-1142.
2. Japan Road Association (1996), *Specification for Highway Bridges* (in Japanese).
3. Kiku, H., Yasuda, S. and Nagase, H. (1995), "Shaking table tests and several analyses on the behavior of buried pipes during liquefaction," *Proceedings, First International Conference on Earthquake Geotechnical Engineering*, 981-986.
4. Matsumoto, H. Sasaki, Y. and Kondo, M. (1987), "Coefficient of subgrade reaction on pile in liquefied ground," *Proceedings, 22nd National Conference on Soil Mechanics and Foundation Engineering*, 827-828 (in Japanese).

5. Trautmann, C.H. and O'Rourke, T.D. (1985), "Lateral force-displacement response of buried pipes," *Journal of Geotechnical Engineering Division, ASCE*, Vol. 111, GT9, 1077-1092.

6. Yasuda, S., Saito, K. and Suzuki, N. (1987), "Soil spring constant on pipe in liquefied ground," *Proceedings, 19th JSCE Conference on Earthquake Engineering*, 189-192 (in Japanese).

7. Yasuda, S., Ishihara, K., Morimoto, I., Orense, R, Ikeda, M., and Tamura, S. (2000), "Large-scale shaking table tests on pile foundations in liquefied ground," *Proceedings, 12th World Conference on Earthquake Engineering*, Auckland, New Zealand, Paper No. 1474, 8pp.

8. Yoshida, T. and Uematsu, M. (1978), "Dynamic behavior of a pile in liquefied sand," *Proceedings, 5th Japan Earthquake Engineering Symposium*, 657-663 (in Japanese).